Supplementary Information (SI) for Materials Chemistry Frontiers.
This journal is © the Partner Organisations 2024

S Defect-rich MoS_2: Differences of S Point-defects and S Stripping-defects in Photocatalysis

Jiafei Ren,[‡a] Jiqi Xing,[‡a] Jian Sun,[a] Haobo Ma,[a] Jiamin You[a] and Juan Liu*[a]

Support Information

Table of Contents

S1. Experimental Details

Materials

Sodium molybdate dihydrate ($Na_2MoO_4 \cdot 2H_2O$, 99 %), thiourea (CH_4N_2S, 99 %), Tert-Butyl alcohol (TBA), p-benzoquinone (PBQ), and methylene blue (MB) were purchased from Shanghai Macklin Biochemical Co., Ltd. Potassium hydrogen phthalate ($C_8H_5KO_4$) was purchased from Sinopharm Chemical Reagent Co., Ltd. Hydrogen peroxide (30 wt %) was purchased from Shenyang Paier Fine Chemicals. Lithium iodide (LiI, 99 %), potassium iodide (KI, ≥ 99 %), ethanol (EA ≥ 99 %), and methanol (≥ 99 %) were acquired from Shanghai Aladdin Biotechnology Co., Ltd. All of these reagents are of analytical grade and can be used directly. The deionized water was self-produced in the laboratory.

Preparation of samples

First, 15 mmol of CH_4N_2S and different amounts of LiI (2 mmol, 4 mmol, 6 mmol, and 8 mmol) were dissolved in 15 mL of deionized water, stirred for 20 minutes, and then 7 mmol of $Na_2MoO_4 \cdot 2H_2O$ was added and stirred for 10 minutes. After stirring evenly, the solution was transferred to a 50 mL polytetrafluoroethylene reaction kettle, sealed, placed in an oven, and reacted at 200 °C for 24 hours. After natural cooling to room temperature, the obtained black precipitate was collected by centrifugation, washed three times with deionized water and anhydrous ethanol, and dried at 60 ℃ for 12 hours. The resulting catalyst was named NMSL-X, where X represents the amount of lithium iodide added.

The pristine MoS_2 was named P-NMS. 15mmol of CH_4N_2S and 7 mmol $Na_2MoO_4 \cdot 2H_2O$ were dissolved in 15mL deionized water, stirred for 30min and then hydrothermal reaction was performed to obtain P-NMS.

Characterization

The structure of the sample was analyzed by X-ray diffractometer (XRD, D/MAX-Ultmer+) equipped with Cu Kα radiation. The UV-Vis absorption spectrum of the sample is determined by UV-Vis spectrophotometer (UV-2700i, SHIMADZU). The morphology and elemental distribution of the samples were analyzed using a scanning electron microscope (SEM, SUPER55/SAPPHIRE) equipped with an energy dispersive spectrometer (EDS). The microstructure of the sample was observed by transmission electron microscopy (TEM, JEM-2100). Analyzing the chemical composition and defect

content of the sample surface using Thermo Scientific K-Alpha photoelectron spectroscopy (XPS). The specific surface area (BET) was measured using a Quantachrome 3.01 specific surface and porosity analyzer. Electron paramagnetic resonance (EPR) spectra were obtained on a Bruker EMX PLUS.

Photocatalytic experiments

Add 30 mg of catalyst to 80 mL of MB solution with a concentration of 10 mg/L, and sonicate for 5 minutes to achieve uniform dispersion. Then, stir for 1 hour in dark to reach adsorption equilibrium. In the subsequent photocatalytic degradation, use a Xenon lamp with a power of 85 mW cm-2 equipped as the light source. During 120 min photocatalytic reaction, collect 3 mL MB solution every 30 minutes, and the supernatant is retained after centrifugation at 11000 rpm. The MB content is determined by measuring the light absorbance intensity of the supernatant at 665 nm. According to Lamber-Beer law, removal rate **η** can be calculated by equation (1). The reaction kinetics of MB degradation is quantitatively characterized by using equation (2).

$$\eta = \left(1 - C_t/C_0\right)\cdot 100\% = \left(1 - A_t/A_0\right)\cdot 100\% \quad (1)$$

$$\ln\left(C_0/C_t\right) = kt \quad (2)$$

Determination of active species

In the active species capture experiment, methanol, Tert-Butyl alcohol (TBA), and p-benzoquinone (PBQ) were used as holes (h^+), hydroxyl radicals (•OH), and superoxide radicals ($\bullet O_2^-$) capture agents, respectively. The capture experiments were carried out with 0.5 mL 0.5 mM capture agents in the photocatalytic degradation reaction system containing 30 mg of catalyst, 80 mL 10 mg/L of MB under light irradiation. The MB concentration was also evaluated as described in Section 1.4.

Electrochemical measurement

Electrochemical measurements were performed in a three electrode system. The test uses Pt wire as the counter electrode, Saturated Calomel Electrode (SCE) as the reference electrode, and a Glassy Carbon Electrode (GCE) coated with a catalyst as the working electrode. The electrolyte used was 0.1 M KCl solution. The EIS in the frequency range of 100 kHz to 0.1 Hz was tested on the ParStat 3000 electrochemical workstation. The transient photocurrent response tests were conducted on the CHI-

660E electrochemical workstation. The power of the light source is 85 mW cm^{-2}, and the illumination interval is 10 s. Testing the MS at a frequency of 1 kHz.

Analysis of photogenerated H_2O_2

The photogeneration of H_2O_2 was detected using a ring-disk electrode (RRDE). Pumping high-purity nitrogen into the deionized water solution for 15 minutes before testing to ensure that the electrolyte is in a nitrogen-saturated state. The disk potential was set at open circuit voltage, and the ring potential was set at 0.9 V vs. SCE. The test is conducted at rotating speed of 1600 rpm and a scan rate of 10 mV s^{-1}.

The concentration of H_2O_2 produced was determined using iodometry. Disperse 30 mg of sample in 80 mL of aqueous solution and sonicate for 5 minutes. After 120 minutes of illumination, 1 mL 0.1 mol L^{-1} $C_8H_5KO_4$ aqueous solution and 1 mL 0.4 mol L^{-1} potassium iodide (KI) aqueous solution were added to 1 mL of centrifuged supernatant. The amount of H_2O_2 is determined by the absorbance of triiodide anions (I_3^-) at 350 nm according to equation (3)

$$H_2O_2 + 3I^- + 2H^+ \rightarrow I_3^- + 2H_2O \quad (3)$$

S2. Simulation Details

The details of the establishment of the water box are described. First, a water cube (31.122 × 31.122 × 30.885 $Å^3$) containing 1,000 water molecules is constructed according to the density (1 g/cm^3) under 101.3 MPa at 298 K. Then it undergoes a relaxation process of 1 ns. The equilibrium water cube were placed on the MoS_2 surface (25.283 × 65.688 $Å^2$). The lattice parameter of MoS_2 models of different S-defect surfaces is 54.590 Å. 1313 water molecules out of the lattice were removed. The establishment of this system model and the above-mentioned relaxation process are all carried out in the Materials Studio.

S3. Supplementary Figures

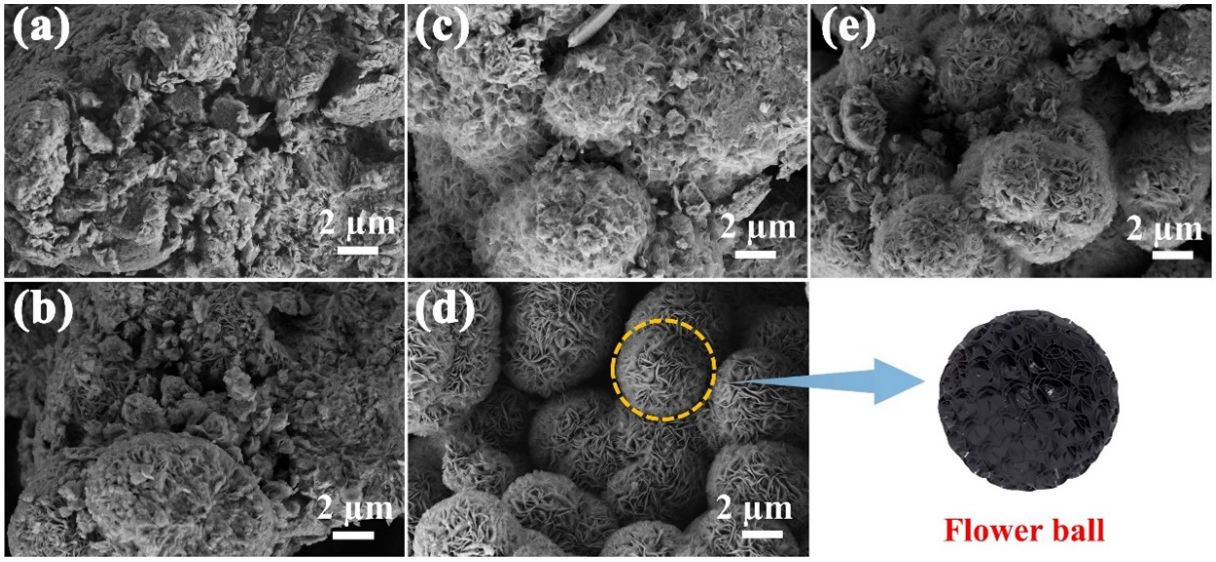

Fig. S1. SEM images of (a) P-NMS (b) NMSL-2, (c) NMSL-4, (d) NMSL-6, and (e) NMSL-8.

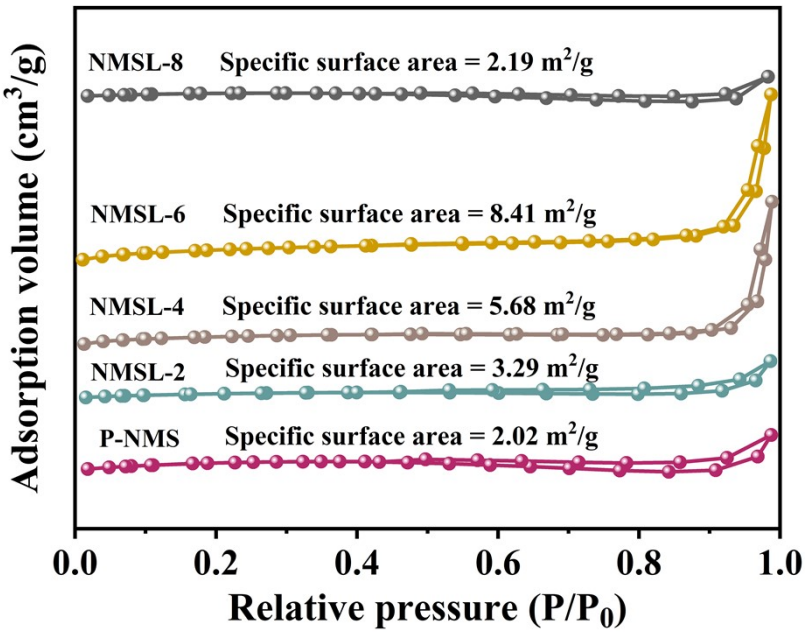

Fig. S2. N_2 adsorption-desorption isotherms

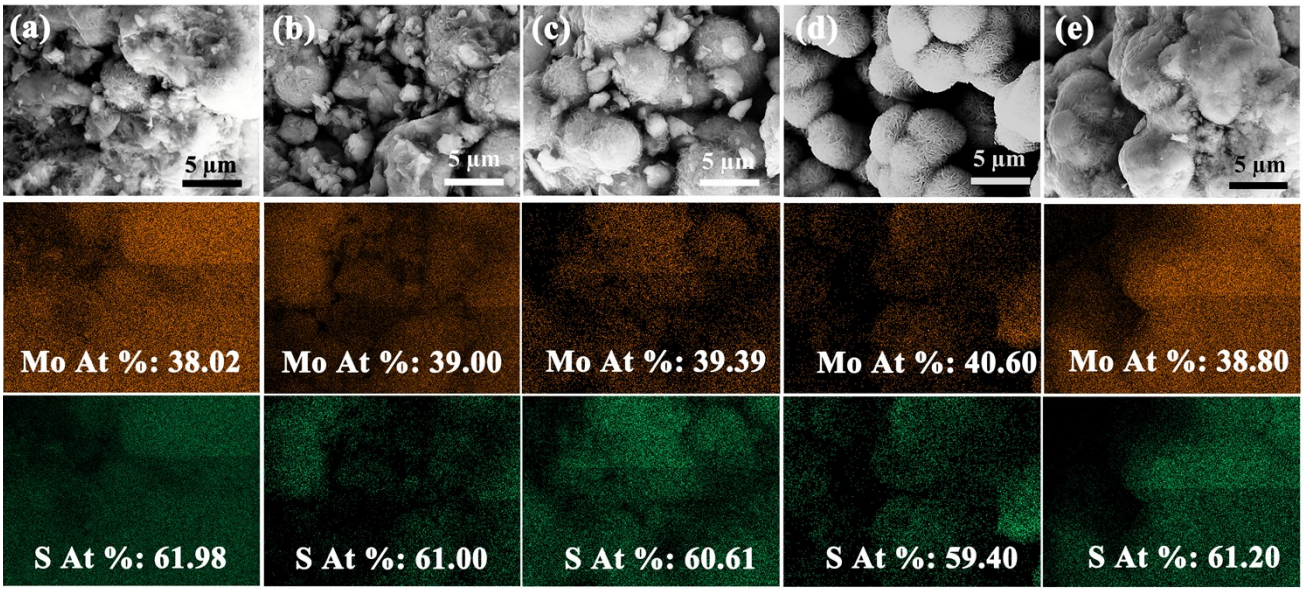

Fig. S3. EDS images of (a) P-NMS, (b) NMSL-2, (c) NMSL-4, (d) NMSL-6, and (d) NMSL-8 and element maps of S and Mo corresponding to this region

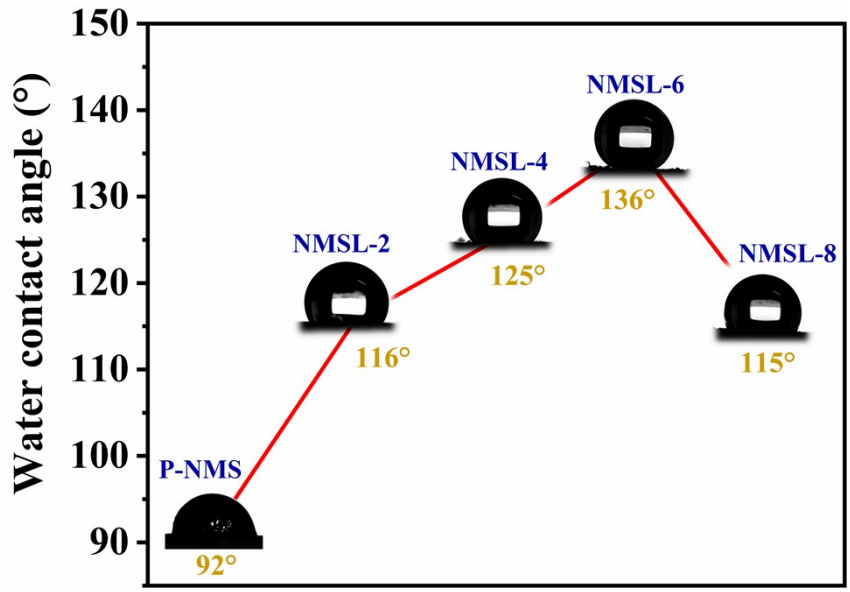

Fig. S4. Water contact angle of P-NMS and NMSL-X.

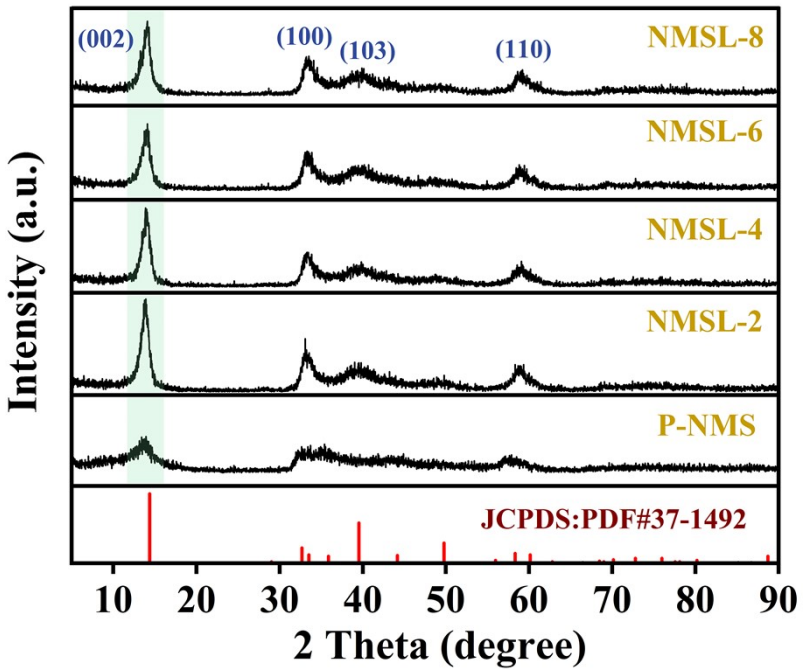

Fig. S5. XRD pattern of P-NMS and NMSL-X.

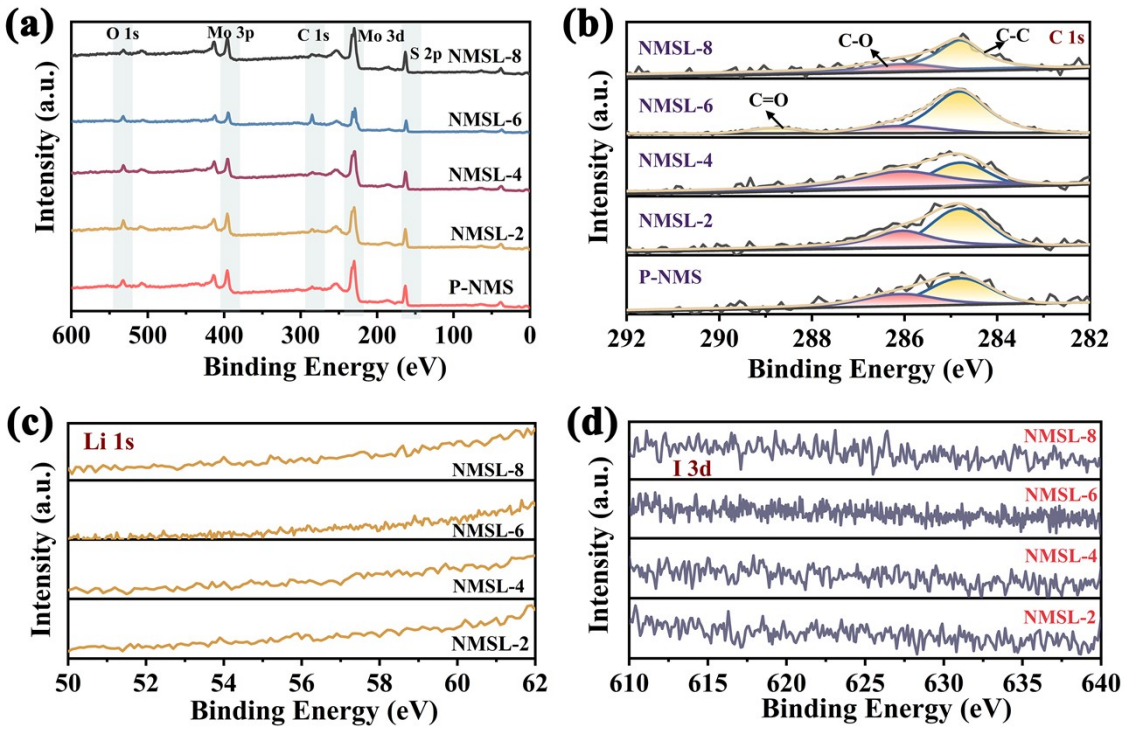

Fig. S6. XPS spectra of P-NMS and NMSL-X. (a) survey spectra, (b) C1s. (c) Li 1s. (d) I 3d.

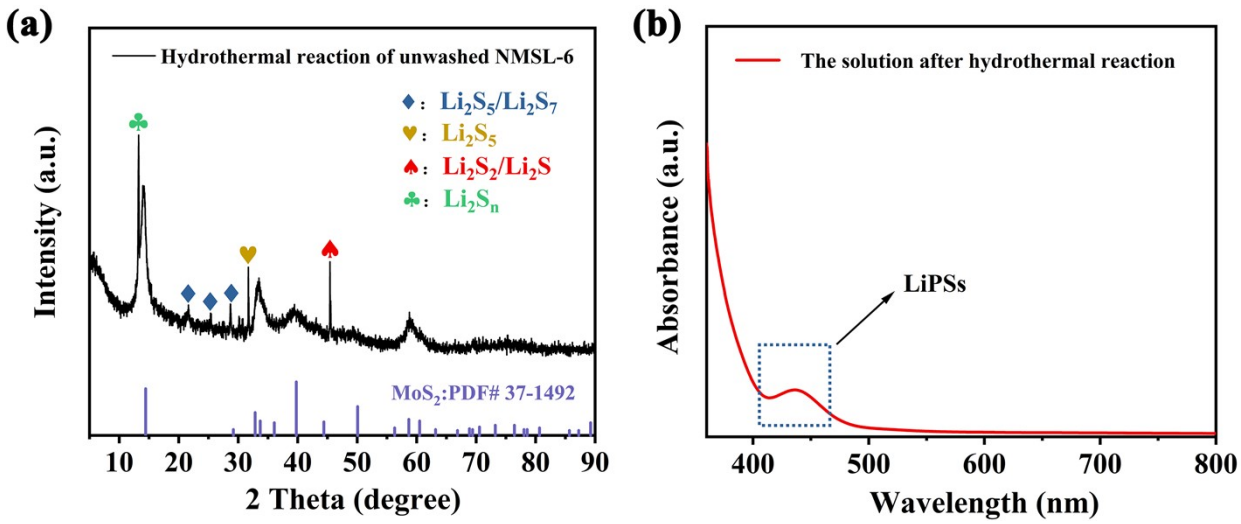

Fig. S7. (a) XRD pattern of unwashed NMSL-6 after hydrothermal reaction. (b) UV-Vis absorption spectrum of the solution after hydrothermal reaction.

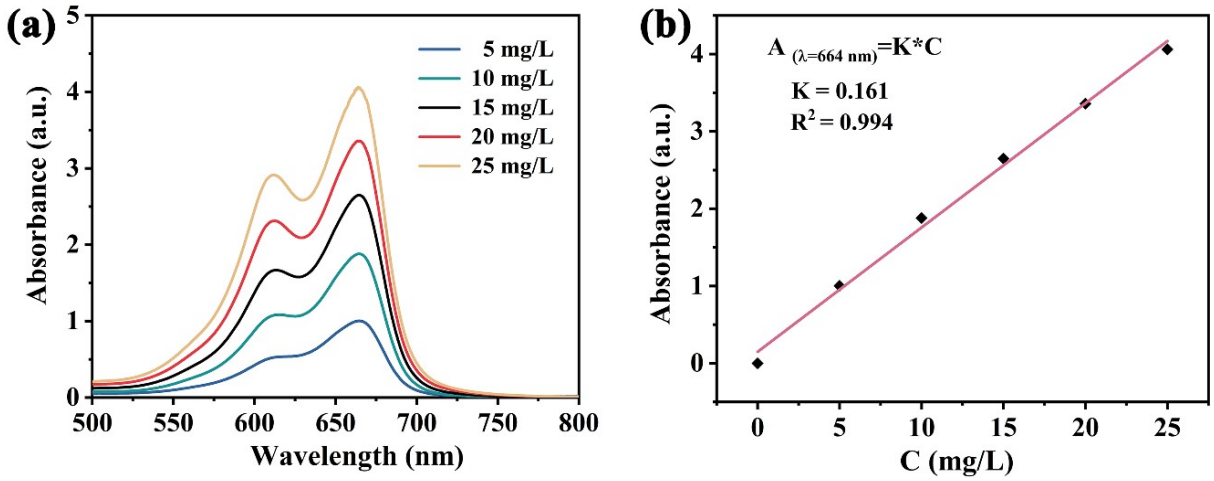

Fig. S8. (a) The absorbance of different concentrations of MB solution at λ=664 nm; (b) standard curve of MB solution concentration versus absorbance

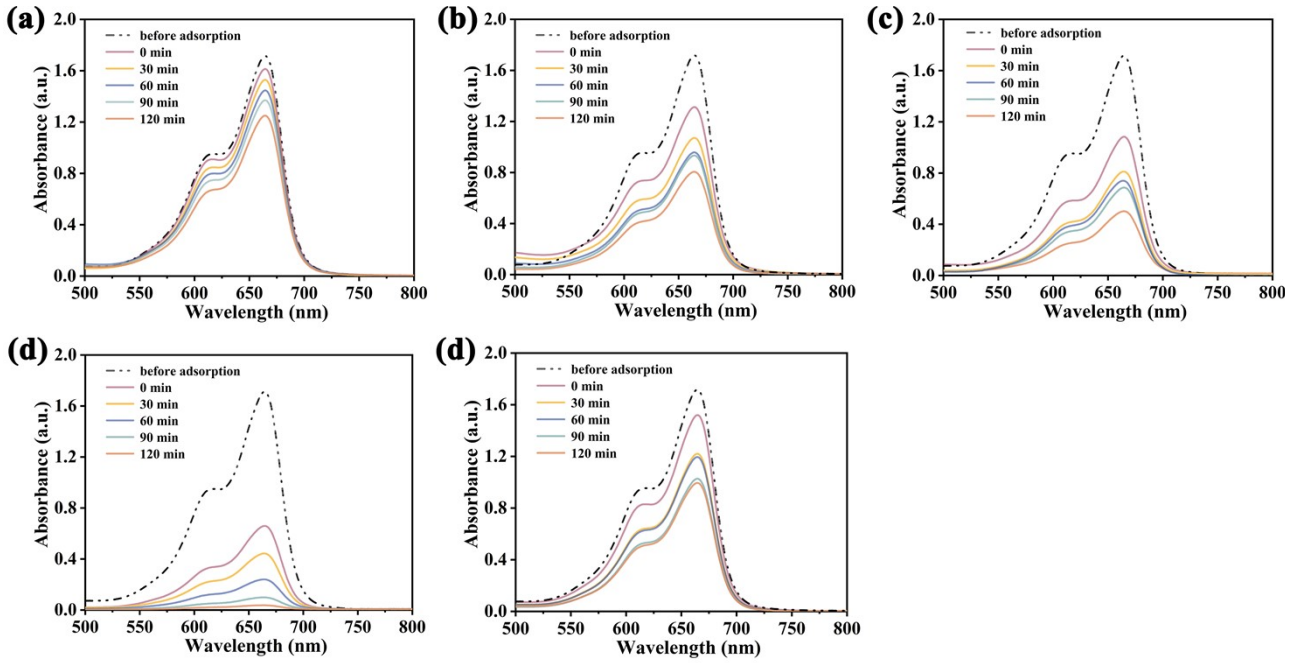

Fig. S9. UV–Vis absorption spectra of MB dye catalyzed by (a) P-NMS, (b) NMSL-2, (c) NMSL-4, (d) NMSL-6, and (e) NMSL-8.

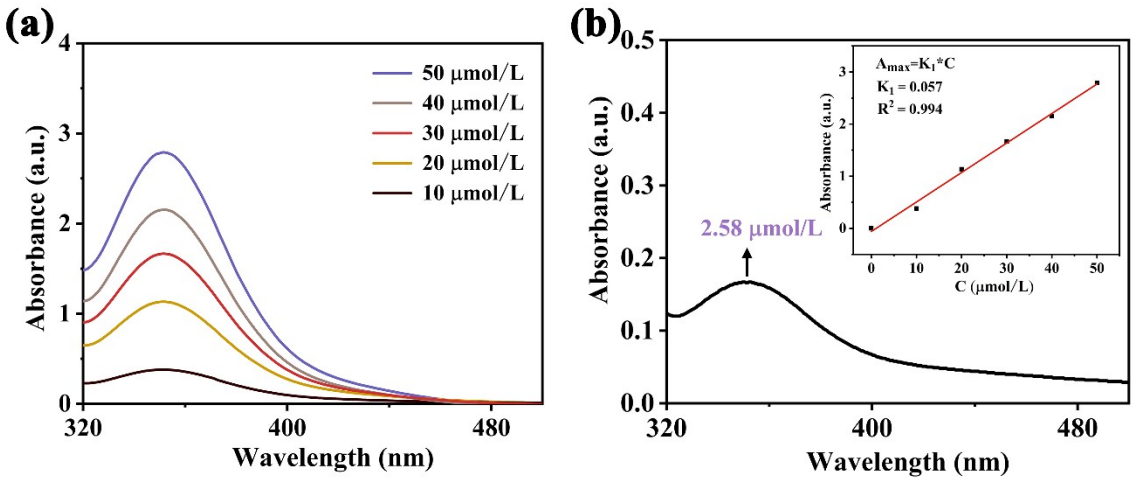

Fig. S10. (a) The UV-Vis absorption spectra of different concentrations of H_2O_2 by iodometry. (b) The H_2O_2 production of NMSL-6 in 2 hours determined by iodometry. The inset shows the calibration curve and fitting equation of H_2O_2 concentration and absorbance.

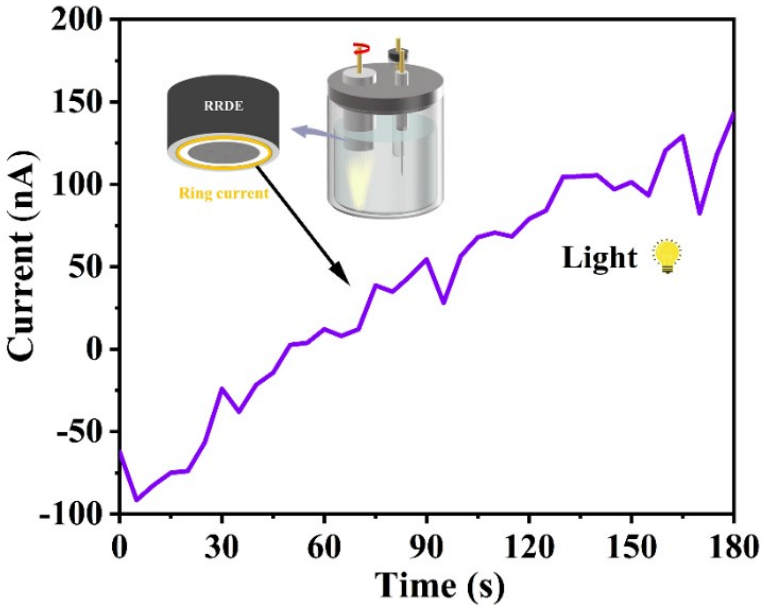

Fig. S11. The ring current time curves in the rotating ring-disk electrode (RRDE) of NMSL-4.

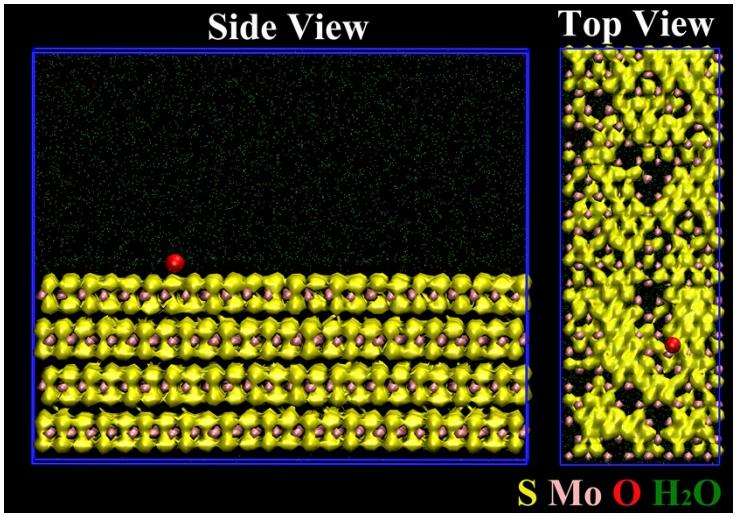

Fig. S12. Model of oxygen adsorption in water on the S point-defects of MoS_2 surface.

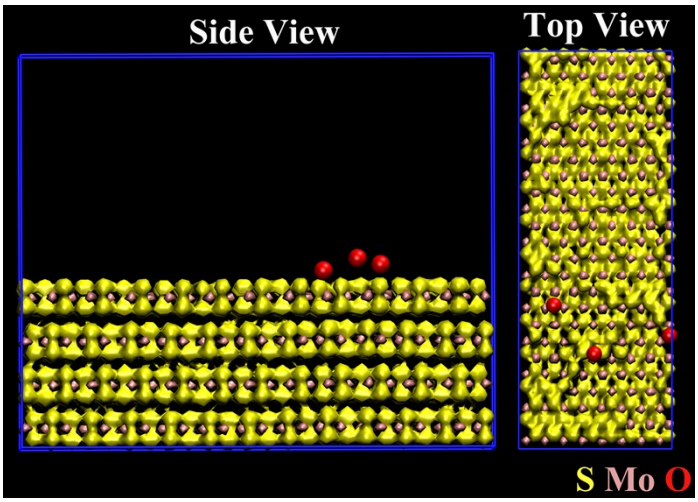

Fig. S13. Model of oxygen adsorption in vacuum on the S stripping-defects of MoS_2 surface.

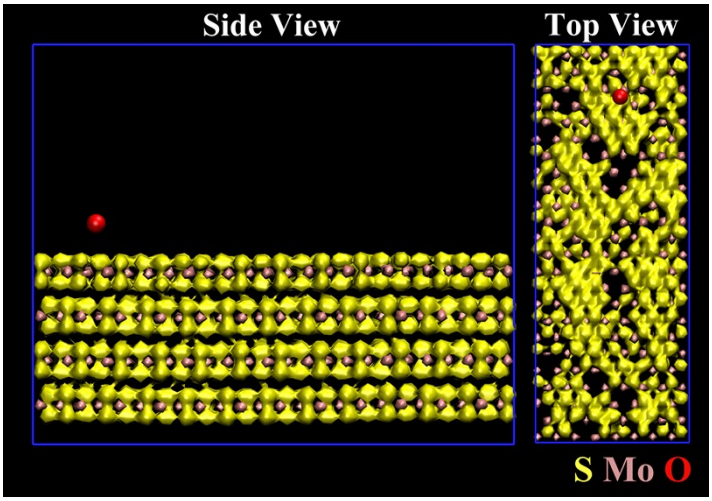

Fig. S14. Model of oxygen adsorption in vacuum on the S point-defects of MoS_2 surface.

S4. Supplementary Tables

Tab S1. Analyzed the content of Mo and S in samples from EDS.

Sample	S/Mo
P-NMS	1.630
NMSL-2	1.564
NMSL-4	1.538
NMSL-6	**1.463**
NMSL-8	1.577

Tab S2. Normalized atomic percentage as determined by XPS.

Sample	S At (%)	Mo At (%)	S/Mo
P-NMS	45.17	24.41	1.85
NMSL-2	38.83	21.45	1.81
NMSL-4	40.42	22.97	1.76
NMSL-6	**17.84**	**11.81**	**1.51**
NMSL-8	46.81	25.72	1.82

Tab S3. Activity of different MoS_2 series catalysts for MB removal.

Sample	activity [mg g^{-1}]	Ref
3% Ag-MoS_2	7.7	[1]
MoS_2/g-C_3N_4	16	[2]
MoS_2@ZnO	23.18	[3]
Mn–SnO_2@MoS_2	15.47	[4]
MoS_2/ CdS	10	[5]
NMSL-6	**26.4**	**This work**

Tab S4. Lattice parameters of the constructed models

Lattice (Å)	a	25.283
	b	65.688
	c	54.590
Cell Angle (°)	α=β=γ	90.000

Supplementary References

1. A. Nazneen, M. I. Khan, M. A. Naeem, M. Atif, M. Iqbal, N. Yaqub and W. A. Farooq, Structural, morphological, optical, and photocatalytic properties of Ag-doped MoS_2 nanoparticles, *Journal of Molecular Structure*, 2020, **1220**, 128735.
2. P. Cao, N. Chen, W. Tang, Y. Liu, Y. Xia, Z. Wu, F. Li, Y. Liu and A. Sun, Template-assisted hydrothermal synthesized hydrophilic spherical 1T-MoS_2 with excellent zinc storage performance, *Journal of Alloys and Compounds*, 2022, **898**, 162854.
3. Y.-H. Tan, K. Yu, J.-Z. Li, H. Fu and Z.-Q. Zhu, MoS_2@ZnO nano-heterojunctions with enhanced photocatalysis and field emission properties, *Journal of Applied Physics*, 2014, **116**.
4. S. Asaithambi, P. Sakthivel, M. Karuppaiah, K. Balamurugan, R. Yuvakkumar, M. Thambidurai and G. Ravi, Synthesis and characterization of various transition metals doped SnO_2@MoS_2 composites for supercapacitor and photocatalytic applications, *Journal of Alloys and Compounds*, 2021, **853**, 157060.
5. S. A. Darsara, M. Seifi and M. B. Askari, One-step hydrothermal synthesis of MoS_2/ CdS nanocomposite and study of structural, photocatalytic, and optical properties of this nanocomposite, *Optik*, 2018, **169**, 249-256.